# COMMENSURATE-LINE, MICROSTRIP, BAND-PASS FILTERS

Moshe Gat

Avantek Inc, 481 Cottonwood Drive
Milpitas, California 95035

ABSTRACT

The commensurate-line, microstrip bandpass filter is a practical topology which yields realizable impedance values for wide-bandwidth filters. Kuroda's network transformations are used to synthesize bandwidth-dependent structures. The distribution of the grounded stub impedances, which is also bandwidth dependent, is discussed in detail for the 40-160% range. The realization of tee-junctions and the method used to ground the stubs are key to this topology. Test results for N=11 filters show excellent correlation between test and simulated data. Sensitivity, phase and temperature stability, rejection of second harmonic and microstrip models are also discussed.

## INTRODUCTION

The commensurate-line bandpass filter topology, also known as the shunt-shorted-stubs topology, has been previously discussed in the literature[1,2]. From the synthesis point of view, a filter from the Nth degree yields a topology with (N-1) series transmission-lines and one stub to ground. (See Figure 1a). Actually, for a network with $Z_{in}=Z_{out}$, in order to maintain symmetry there is one stub to ground if N is odd and two grounded stubs if N is even.

This canonical topology is unique. However, for most practical applications the impedance levels are not realizable, i.e. line impedances of one ohm or less. The problem of the grounded stub's unrealizable impedance level can be solved. By applying the Kuroda's network transformations (N-1) times the filter topology is converted into the one shown in Figure 1b. The transformations distribute the stub's impedance along the filter so that there are N shorted stubs separated by (N-1) series transmission lines. The filter topology for N=7 is shown in Figure 1b where all the elements are quarter-wavelength long at the arithmetic center frequency $F_0=(F_h+F_l)/2$.

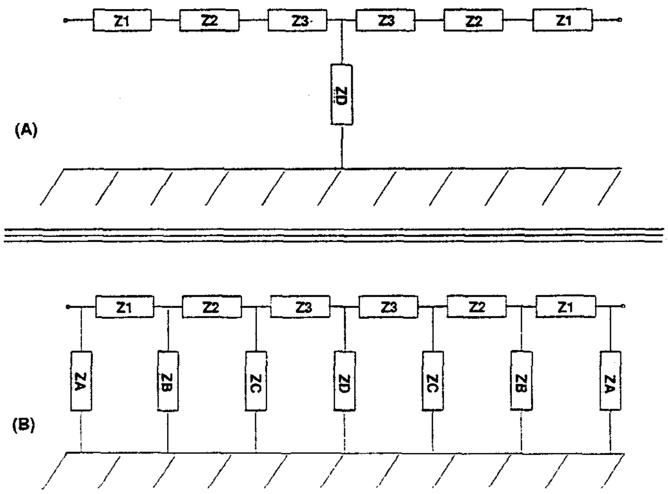


FIGURE 1: Commensurate line bandpass filter, N=7

## THE TOPOLOGY

The application of Kuroda's transformations is not unique. One can use different transformation ratios to create many impedance distributions across the topology. For a topology of the Nth degree the transformations are applied N-1 times. It is possible to solve this set of nonlinear Kuroda's equations so that all stubs to ground have the same impedance level. Referring to the N=7 schematic in Figure 1 this means: $Z_a=Z_b=Z_c=Z_d$. Using this solution we can now make a table of the impedance levels as a function of bandwidth, and determine the region of validity for this topology.

The bandwidth in Table 1 is the equal ripple bandwidth. The region of validity for a given printed filter topology is a function of dielectric constant, thickness of the dielectric and the range of line width that one can realize. This means that the topology's range of validity depends on the selection of the dielectric material and the quality of the thin film processing. In any event, for alumina with $E_r=9.8$ and dielectric thickness of 10, 15 & 25 mils it is clear from Table 1 that the topology yields very realizable impedance values for bandwidth of 50 to 110%. The range could be extended mainly by using different dielectric materials. For example, the use of fused silica with a dielectric constant of 3.78 will extend the high end of the bandwidth range.

At this point we can look at the impedance values of Table 1 and draw some more conclusions. First, the values of the series transmission lines change rather slowly and are always very reasonable. Second, we observe that most of the "action" takes place with the impedances of the grounded stubs. The impedance value decreases as we lower the bandwidth and increases as we raise the bandwidth. It is easy to understand this trend if we remember that this is a distributed structure. Actually the filter is a microwave high-pass filter with cut-off frequency at



0149-645X/88/0000-0423$01.00 © 1988 IEEE

$F_1$ of the band-pass filter and quarter wave frequency at our $F_0$. The wider the bandwidth, the more this filter looks like an "ideal" high-pass filter. As we converge into a more high-pass characteristic, we need ever smaller values of distributed capacitance to ground. Hence the stub's impedance increases, which corresponds to narrower microstrip lines and therefore smaller capacitance to ground. As we change the bandwidth the other way, towards lower values, the opposite effect takes place. We need ever increasing capacitance to ground, and hence the stub impedances decrease.

IMPEDANCE MATRIX , N=7

| BW [%] | $Z_1$ | $Z_2$ | $Z_3$ | $Z_g$ |
|---|---|---|---|---|
| 40.0 | 50.10 | 62.37 | 67.57 | 17.56 |
| 50.0 | 49.00 | 59.73 | 64.92 | 23.87 |
| 60.0 | 47.94 | 57.14 | 62.13 | 31.42 |
| 70.0 | 46.94 | 54.61 | 59.24 | 40.59 |
| 80.0 | 45.99 | 52.14 | 56.26 | 51.98 |
| 90.0 | 45.10 | 49.77 | 53.23 | 66.51 |
| 100.0 | 44.28 | 47.52 | 50.23 | 85.62 |
| 110.0 | 43.53 | 45.43 | 47.34 | 111.73 |
| 120.0 | 42.88 | 43.56 | 44.69 | 149.13 |

TABLE-1

* $Z_g=Z_a=Z_b=Z_c=Z_d$

The above discussion about the relationship between bandwidth, capacitance and stub impedance yields the idea that one can extend the useable range of the filter topology by controlling the number of the grounded stubs. As the bandwidth gets higher, the number of grounded stubs can be gradually reduced to compensate for the need for lower equivalent capacitance to ground. Trying to extend the range into lower bandwidth, one can transform the impedances to higher values and then split the input/output stubs. Table 2 shows how changing the number of grounded stubs extends the useful range of the topology to 40-160%. Figure 2 a,b,c,d,e,f shows the topologies of N=7, $f_0$=10 GHz, 0.1 dB Tchebycheff filters for bandwidths of 40, 70, 100, 120, 140, and 160% respectively.

IMPEDANCE MATRIX, N=7

| BW % | $Z_1$ | $Z_2$ | $Z_3$ | $Z_a$ | $Z_b$ | $Z_c$ | $Z_d$ |
|---|---|---|---|---|---|---|---|
| 40.0 | 63.4 | 100.0 | 108.4 | D-32.7 | 31.1 | 28.2 | 28.2 |
| 70.0 | 46.9 | 54.6 | 59.2 | 40.6 | 40.6 | 40.6 | 40.6 |
| 100.0 | 44.3 | 47.5 | 50.2 | 85.6 | 85.6 | 85.6 | 85.6 |
| 110.0 | 31.3 | 23.5 | 24.5 | ---- | 33.7 | 57.9 | 57.9 |
| 120.0 | 33.3 | 24.0 | 22.0 | ---- | 61.9 | 61.9 | 61.9 |
| 130.0 | 35.1 | 32.6 | 34.5 | ---- | 59.3 | ---- | 91.9 |
| 140.0 | 36.8 | 37.7 | 48.2 | ---- | 73.7 | ---- | ---- |
| 150.0 | 38.2 | 28.8 | 25.4 | ---- | ---- | 90.2 | ---- |
| 160.0 | 39.6 | 32.6 | 25.4 | ---- | ---- | ---- | 74.2 |
| 170.0 | 40.7 | 36.0 | 31.1 | ---- | ---- | ---- | 163.8 |

TABLE-2

* $Z_a$ is a split ("doubled") impedance for BW=40 [%]

Looking at the filter drawings of Figure 2, three key topological details are obvious.

1 The grounded stubs alternate up and down.
2 Special care is taken to realize the tee-junction area.
3 Special care is taken to realize the stub grounds.

These lay out details are the key to a successful implementation of the topology.

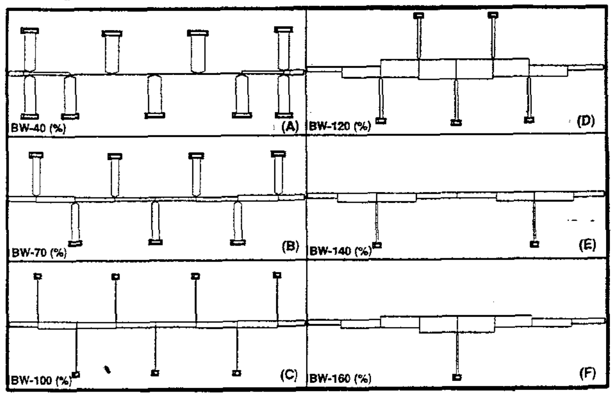


FIGURE 2: Layout details

Alternating the stubs is a must in order to keep the parasitic coupling between the stubs as small as possible i.e. half a wave length. Test results have shown that placing all grounded stubs on the same side yields unacceptable degradation in performance due to a quarter-wave length parasitic coupling.

Tee-junction details are shown in Figure 3. The step discontinuity is taken away from the junction to the "other-side". A tiny connecting segment provides good junction plane definition. The tapering segment compensates, to a degree, for the parasitics of the junction.

The ground planes for the stubs are realized with slots. Wide slots provide negligible equivalent resistance and inductance. The slots also provide a ground plane as opposed to a grounded point, as in the case of a via hole. The equivalent stub length L is also shown in Figure 3.

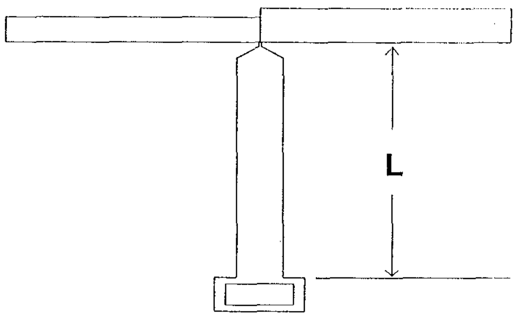


FIGURE 3: Tee-junction detail

## TEST RESULTS

Many different filters have been realized on 10, 15, 25 and 50 mil alumina. Some filters were printed on 10 and 15 mil fused silica. The in-band response of an N=11 6-12 GHz filter is shown in Figure 4. The insertion loss is 0.7 dB and the full 11 spikes of the return loss are apparent. Note the good agreement with the simulated results, Figure 4 a, b.

Figure 4c shows the same filter. Note that the ultimate rejection is better than 60 dBc and the parasitic second harmonic response, at about 17.5 GHz, is suppressed to 50 dBc. Figure 5 shows an N=9, 6-18 GHz filter and Figure 6 shows an N=11, 12-18 GHz filter. The slope of the filter's skirts is a function of N and the shape factor. Hence the skirts in Figure 6 are much steeper than the ones in Figure 5, since the corresponding bandwidths are 40 and 100%.

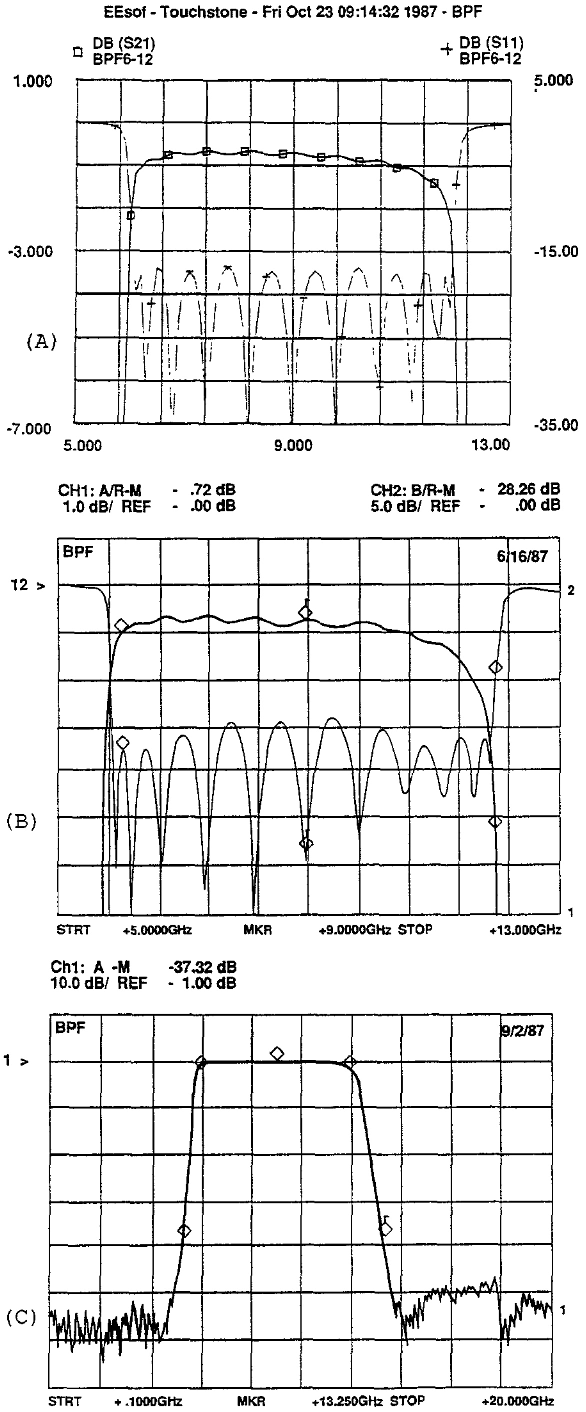


FIGURE 4: Filter response, N=11, 6-12 GHz

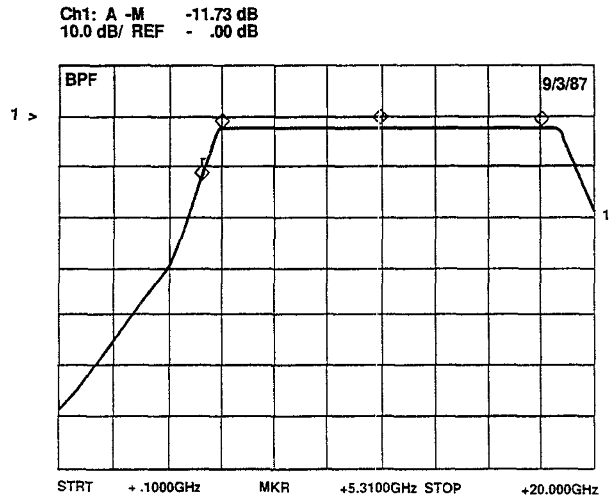


FIGURE 5: Filter response, N=9, 6-18 GHz

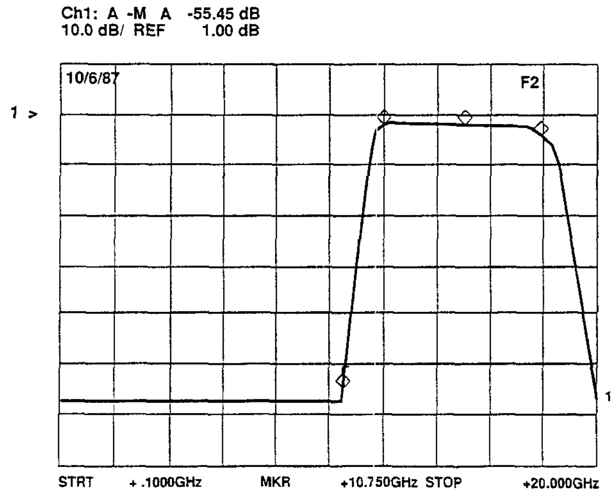


FIGURE 6: Filter response, N=11, 12-18 GHz

## SENSITIVITY, MICROSTRIP MODELS, PHASE and TEMPERATURE EFFECTS

The real key to a successful implementation of this filter topology is to pay very careful attention to all the details.

First, full direct synthesis is needed, because optimized impedance values will yield poor second harmonic suppression. Second, an excellent microstrip model is needed. A less than perfect model will yield weak suppression of the second harmonic and a poor in band return loss. We use Hammerstad & Jensen[3] for a static model and for metallization thickness correction, Kirschning & Jensen[4] for dispersion, and Getsinger[5] for the application of the dispersion to the characteristic impedance. It is also assumed that an excellent thin-film process yielding very precise control of the metallized dimensions is used.

Third comes the issue of alignment between the drilled slots and the metallization. If the two were misaligned by +/-2 mil as shown in Figure 7, the degradation of the in-band return loss is shown in Figure 8. We assume that tight control over the distribution of Er is in place. Precise and repeatable Er is a key for good phase repeatability. If alumina is the material of choice $E_r$= 9.8 +/-0.1 is not good enough for phase specs.

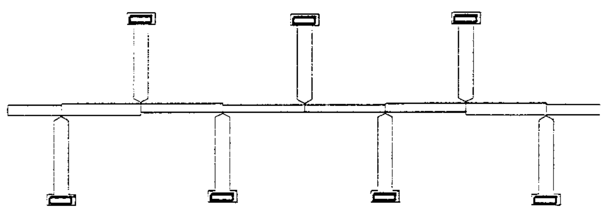

FIGURE 7: Misalignment between drilled slots and metallization

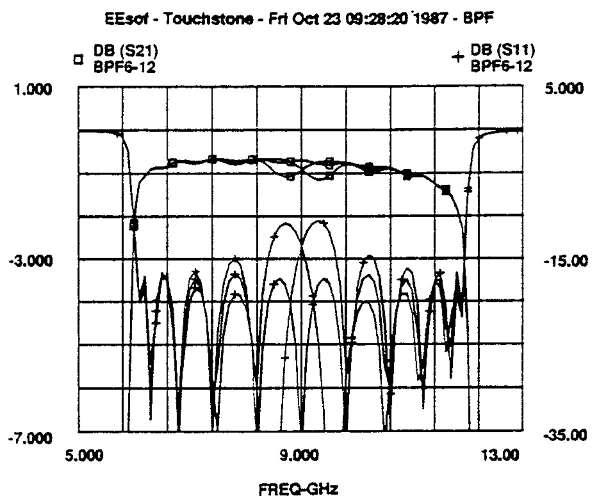


FIGURE 8: Performance degradation due to misalignment

Finally, looking at the filter's performance over temperature, we are limited by the fundamental properties of the dielectric material. Using either alumina or fused silica, both with low thermal coefficient of expansion and very low $D_{Er}/D_{Temp}$, (136 ppm/°C for alumina), the filter barely drifts over temperature. Because these are wide bandwidth filters by definition, the drift in response is so small that we could hardly detect any in our tests.

PROBLEMS, AREAS for FUTURE IMPROVEMENTS

Though we found the commensurate-line topology extremely useful, there are some areas where improvements can be made.

First, the junction can be improved so that it approaches the ideal "parasitic free" tee-junction. An improved junction should reduce the level of worst-case return loss, and suppress the second harmonic response even further.

The second potential improvement is in the low bandwidth end of this topology, around 40%, where the input/output stubs are split (see Figure 2a). The impedance split has much stronger parasitic coupling, quarter- vs half-wave-length. This added coupling stores energy, causes reduced bandwidth and degrades in-band return loss and insertion loss. Taking this extra coupling into account in the synthesis stage will improve the response.

Finally the topology outlined in Table 1 uses the same impedance for all grounded stubs. However, this equal impedance level is not critical in terms of performance. It is possible to use the transformations so that all series transmission lines are equal. See Table 3 for comparison between the two topologies for N=5. This alternate topology has the advantage of minimizing discontinuity effects and "simplifying" the tee-junction.

EQUAL-STUBS VS EQUAL-LINES TOPOLOGIES, N=5

| BW [%] | $Z_1$ | $Z_2$ | $Z_a$ | $Z_b$ | $Z_c$ |
|---|---|---|---|---|---|
| | 47.33 | 54.27 | 33.17 | <---- | <---- |
| 60.0 | | | | | |
| | 41.27 | <---- | 36.97 | 23.14 | 25.22 |
| | 45.26 | 49.06 | 55.99 | <---- | <---- |
| 80.0 | | | | | |
| | 41.75 | <---- | 62.49 | 43.47 | 47.64 |
| | 43.54 | 44.77 | 95.03 | <---- | <---- |
| 100.0 | | | | | |
| | 42.35 | <---- | 101.24 | 84.84 | 89.90 |

TABLE-3

SUMMARY

The commensurate-line filter topology is a practical solution for realization of medium to wide bandwidth filters. Excellent correlation between test and simulated data allows the designer to realize high order polynomials. A fully computerized generation of these filters allows a non-filter-expert to make a complex filter that works as predicted in the first attempt.

ACKNOWLEDGMENT

I would like to thank Thomas A. Riso for writing software that generates these filter designs automatically.

REFERENCES

[1] Matthaei, G.L.,Young, L.,and Jones, E.M.T., Design of Microwave Filters, Impedance-Matching Networks and Coupling Structures. New York: McGraw-Hill 1964.

[2] Malherbe,J.A.G., Microwave Transmission Line Filters. Artech House 1979

[3] Hammerstad, E., and Jensen, O.,. "Accurate Models for Microstrip Computer-Aided design." MTT Symposium Digest, 1980.

[4] Kirschning, M., and Jansen, R.H. "Accurate Model for Effective Dielectric Constant of Microstrip with Validity up to Millimetre-Wave Frequencies." Electronics Letters, 1982.

[5] Getsinger, W.J. "Measurement and Modeling of the Apparent Characteristic Impedance of Microstrip." MTT-31, August 1983.